DALTON

Quasi-one-dimensional bis(ethylenedithio)tetrathiafulvalene charge-transfer salts with paramagnetic Group 6 anions*

Cameron J. Kepert,[a] Mohamedally Kurmoo,[a] Mary R. Truter[b] and Peter Day[a]

[a] *Davy Faraday Research Laboratory, The Royal Institution, 21 Albemarle Street, London W1X 4BS, UK*
[b] *Department of Chemistry, University College, 20 Gordon Street, London WC1H 0AJ, UK*

Two new charge-transfer salts of BEDT-TTF [bis(ethylenedithio)tetrathiafulvalene] with paramagnetic anionic complexes of Group 6 elements have been prepared. The crystal structure of the salt [BEDT-TTF][$MoOCl_4(H_2O)$] is unusual in containing no segregated layers of cations and anions but chains of hydrogen-bonded $[MoOCl_4(H_2O)]^-$ sandwiched between ribbons of $BEDT\text{-}TTF^+$ edge linked by S···S contacts. The structure of $[BEDT\text{-}TTF]_2[Cr(NCS)_4(NH_3)_2]$ consists of alternating layers of $[(BEDT\text{-}TTF)_2]^+$ and $[Cr(NCS)_4(NH_3)_2]^-$. The molecular packing in the cation layer is unique in comprising double stacks which alternate in orientation with close S···S contacts not only between cations but between cations and NCS. Both compounds are semiconductors and their magnetic behaviour is dominated by the anions, though there is evidence that the cation ribbons in the molybdenum salt behave as antiferromagnetic chains ($J \approx 110$ K).

There are many physical phenomena specific to lattices in which the dominant interactions between the repeating units occur in only one dimension. Examples are the absence of long-range magnetic order above absolute zero and the instability of a one-dimensional electron gas. Owing to this there have been sustained efforts to synthesize new materials with structures that support one-dimensional interactions.[1] For example, there are two main families of highly conducting one-dimensional materials: molecular charge-transfer salts based on the tcnq† acceptor molecule *e.g.* ttf·tcnq[2] and doped salts of square-planar Group 10 transition-metal anions *e.g.* $K_2[Pt(CN)_4]Br_{0.3}\cdot 3H_2O$.[3,4] Both families of material undergo transitions to the semiconducting state at low temperature.

In addition, some charge-transfer salts of BEDT-TTF [bis(ethylenedithio)tetrathiafulvalene] have quite strongly one-dimensional properties in spite of having structures containing alternating layers of BEDT-TTF cations and inorganic anions. The two new compounds of this kind that form the subject of the present paper, [BEDT-TTF][$MoOCl_4(H_2O)$] and [BEDT-TTF]$_2$[$Cr(NCS)_4(NH_3)_2$], have the additional characteristic of containing only one crystallographically independent BEDT-TTF molecule. Furthermore, they contain paramagnetic anions and so offer the opportunity of studying the interaction between two spin systems. We report the synthesis, crystal structure, electronic transfer integrals and physical properties of these compounds.

Experimental

Syntheses

[NEt_4][$MoOCl_4(H_2O)$]. This compound was prepared by modification of the method of Bino and Cotton[5] for the synthesis of [NEt_4][$MoOBr_4(H_2O)$]. The compound $Mo_2(O_2CMe)_4$ and NEt_4Cl (1.69 g) were dissolved in concentrated hydrochloric acid (40 cm^3) with heating in air. The solution was evaporated to low volume with the continuous passing of gaseous hydrogen chloride, and then allowed to cool. The brick-red crystals were collected and recrystallised from concentrated hydrochloric acid.

[NEt_4][$MoOCl_4$]. This compound was prepared by the above procedure but with the continued flow of gaseous hydrogen chloride while cooling the solution. Pale green needles were obtained. Recrystallisation from CH_2Cl_2 and diethyl ether produced large transparent green block-like crystals.

[NBu^n_4][$Cr(NCS)_4(NH_3)_2$]. This compound was prepared by metathesis. Ethanolic aqueous solutions of $[NH_4][Cr(NCS)_4(NH_3)_2]\cdot H_2O$ (2.1 g; Aldrich, 93+%) and NBu^n_4OH (3.8 g) were mixed, and the red precipitate was recrystallised from dichloromethane and diethyl ether to produce large, deep red plates.

Crystal growth

Crystals were grown electrochemically in H-shaped cells (45 cm^3 capacity) under constant-current conditions. On oxidation of BEDT-TTF in solution crystals grew on the platinum anode. The compound BEDT-TTF (*ca.* 20 mg), twice recrystallised from $CHCl_3$, was added to the anode section of the cell, and a solution of the anion salt (*ca.* 20 mg) was added to all three compartments. The cells were set up under an atmosphere of dry Ar and placed in a dark enclosure on a vibration-free table. Using [NEt_4][$MoOCl_4(H_2O)$] as supporting electrolyte in a solvent of 1,1,2-trichloroethane at currents of 0.5 and 1.0 μA, moderately thin black plates which stacked on one another grew on the anode. When the solvent was dichloromethane and the current 0.3 and 0.5 μA, high-quality, black needles formed. Similarly with benzonitrile as solvent and current of 0.5 μA, moderately thick, black needles of high quality formed on the anode.

To grow crystals of the [$Cr(NCS)_4(NH_3)_2$] salt of BEDT-TTF, both the NBu^n_4 and NH_4 salts of the anion were employed. In order to use $[NH_4][Cr(NCS)_4(NH_3)_2]\cdot H_2O$ as supporting electrolyte it was doubly recrystallised from an ethanol–water mixture to produce clear red, block-like crystals, which were finely ground prior to inclusion in the electrochemical cells, to aid dissolution. With dichloromethane as solvent, 18-crown-6 (1,4,7,10,13,16-hexaoxacyclooctadecane) to solubilise the salt and a current of 0.5 μA, large, high-quality, black platelets of [BEDT-TTF]$_2$[$Cr(NCS)_4(NH_3)_2$] and a black polycrystalline, fibre-like coating formed on the anode.

* *Non-SI unit employed*: eV ≈ 1.60×10^{-19} J.
† tcnq = Tetracyanoquinodimethane, ttf = tetrathiafulvalene = 2-(1,3-dithiol-2-ylidene)-1,3-dithiole.

Crystallography

[BEDT-TTF][$MoOCl_4(H_2O)$]. Preliminary X-ray oscillation and Weissenberg studies showed that the long axis of the crystals corresponded to the crystallographic *a* axis. The crystal, sealed in a Lindeman glass capillary, was mounted at room temperature on an automated four-circle Nicolet R3mV diffractometer with graphite-monochromated Mo-Kα radiation (λ = 0.70 783 Å). The unit cell was determined and least-squares refined from 25 independent reflections in the range $19.5 \leqslant 2\theta \leqslant 22°$, in agreement with the X-ray photographic studies. Monitoring of the standard reflections (3, 1, $\bar{2}$), (1, 2, 4) and ($\bar{1}$, $\bar{3}$, 2) during the collection of a full hemisphere of data (2117 reflections) indicated a smooth and equal decrease in intensities to 93%, probably because of irradiation damage.

Structure solution was complicated by the presence of disorder in the Mo atom. Phase generation by the heavy-atom method with a Mo atom on an inversion centre was unsuccessful in generating other atomic positions, and the structure was eventually solved by the location of S–S vectors in the Patterson map. Ethylene group hydrogen atoms were located in the Fourier-difference map, and their positions refined with fixed isotropic thermal parameters. The hydrogen-bonding H atom of the anion (with 50% occupation) was located in the difference map. The data were corrected for absorption by the ellipsoidal empirical method, having collected nine ψ-scan reflection data. The correction led to a significantly lower *R* factor: for example, for reflections from the full data set with $I \geqslant 2\sigma(I)$, $R = 0.061$ without and 0.059 with correction. No reflections were omitted on the grounds of extinction. Further details of the data collection, processing and structural refinement may be found in Table 1.

[$(BEDT\text{-}TTF)_2[Cr(NCS)_4(NH_3)_2]$]. Room-temperature oscillation and Weissenberg photographs using Mo-Kα radiation showed no satellite reflections or diffuse scattering. The *b* axis was found to correspond to the long axis of the crystal plates, which form perpendicular to the *a* axis. The crystal, sealed in a Lindeman glass capillary, was mounted on an automated four-circle Nicolet R3mV diffractometer with graphite-monochromated Mo-Kα radiation. The unit cell was least-squares refined from 25 independent reflections in the range $17.0 \leqslant 2\theta \leqslant 26.7°$. The structure was refined without correcting for absorption, no strongly under-observed reflections being found.

All structure refinements were based on *F*, using the SHELXTL PLUS suite of programs.[6]

Atomic coordinates, thermal parameters, and bond lengths and angles have been deposited at the Cambridge Crystallographic Data Centre (CCDC). See Instructions for Authors, *J. Chem. Soc., Dalton Trans.*, 1997, Issue 1. Any request to the CCDC for this material should quote the full literature citation and the reference number 186/358.

Electrical conductivity

Conductivity measurements were made on [BEDT-TTF][$MoOCl_4(H_2O)$] using conventional two- and four-probe methods both along and through the crystal. Four-probe measurements on $[BEDT\text{-}TTF]_2[Cr(NCS)_4(NH_3)_2]$ were made along the *b* axis. The temperature was varied from 77 to 300 K with an Oxford Instruments CF200 continuous-flow cryostat.

Magnetic measurements

The salt [BEDT-TTF][$MoOCl_4(H_2O)$] was placed in one of a series of gelatine capsules inside a plastic drinking straw inserted into a Quantum Design MPMS 7 SQUID magnetometer. Susceptibility data were collected with an applied field of 0.05 T from 2 to 300 K, and magnetisation at 5 K with fields from 0.005 to 7 T. The salt $[BEDT\text{-}TTF]_2[Cr(NCS)_4(NH_3)_2]$ was mounted in a Perspex rod in the SQUID magnetometer. Susceptibility data were collected with an applied field of 1 T from 2 to 300 K, and magnetisation data with applied fields from 0.1 to 7 T at temperatures of 2 and 5 K. No superconducting or ferromagnetic impurities were detected.

Infrared reflectivity

The reflectivity of the large faces was measured on the plate-like crystals of both compounds using a spectrometer equipped with a microscope. The reflectivity of the smaller face of [BEDT-TTF][$MoOCl_4(H_2O)$] was measured on a thick needle crystal.

Electronic band structure

Band-structure calculations were performed in the tight-binding formalism within the dimer-splitting approximation using the extended-Hückel method, with a double-zeta basis set.[4]

Results and Discussion

Crystal structures and electronic band structures

[BEDT-TTF][$MoOCl_4(H_2O)$]. The phase [BEDT-TTF][$MoOCl_4(H_2O)$] was the sole product of electrocrystallisation from solutions containing $[MoOCl_4(H_2O)]^-$ in three different solvents. Solutions containing $[MoOCl_4]^-$ in the same three solvents gave no product until water was added, when crystals of [BEDT-TTF][$MoOCl_4(H_2O)$] formed, suggesting that the hydrogen-bonded anion chains are important in the energetics of crystal growth.

The salt [BEDT-TTF][$MoOCl_4(H_2O)$], which crystallises in the triclinic space group $P\bar{1}$, has the second smallest unit-cell volume of all known BEDT-TTF salts ($U = 523.0$ Å^3 compared to 424.4 Å^3 for [BEDT-TTF][$CuCl_2$][7]). The asymmetric unit contains one half of $BEDT\text{-}TTF^+$ [centred on the (0, 0, $\frac{1}{2}$) inversion centre] and 50% occupation of the $[MoOCl_4(H_2O)]^-$ anion, which randomly occupies one of the two inversion-related positions about ($\frac{1}{2}$, $\frac{1}{2}$, $\frac{1}{2}$). The structure is unusual in not containing discrete layers of cations and anions, but chains of hydrogen-bonded anions sandwiched between edge-linking ribbons of BEDT-TTF (Fig. 1). The packing arrangement is reminiscent of that of [BEDT-TTF][$Re_6Se_5Cl_9$]·2dmf[8,9] (dmf = dimethylformamide) in which uniform ribbons of $BEDT\text{-}TTF^+$ are separated by the large diamagnetic cluster anion. Isolated uniform one-dimensional stacks of $BEDT\text{-}TTF^+$ have also been observed in [BEDT-TTF][$AuCl_2Br_2$].[10] There is no hydrogen-bonding between the anion and the donor CH_2 groups with all Cl···H distances exceeding 2.85 Å. Selected intramolecular bond lengths and angles are listed in Table 2.

Ribbons of BEDT-TTF are formed by the side-to-side interaction of neighbouring molecules along the *a* direction with short intermolecular S···S distances. The shortest S···S distances between ribbons are those between the ends of the molecules (3.59–3.94 Å). The structure is an addition to the rare group of BEDT-TTF charge-transfer salts in which each donor molecule carries an unambiguous charge of +1. The CH_2 groups of the donor are well ordered in the chair configuration, with a torsion angle S(3)–C(4)–C(5)–S(4) of 67.8(7)°, while the inversion symmetry dictates the conformation of the BEDT-TTF as staggered.

The chains of $[MoOCl_4(H_2O)]^-$ along the *a* direction are formed by hydrogen bonding between the H_2O and O of anions in neighbouring cells. Each chain is oriented with the H_2O projecting either along the positive or negative *a* direction. There is no crystallographic evidence for correlation between neighbouring chains: intensity statistics indicate a centrosymmetric cell (*i.e.* $P\bar{1}$ not $P1$), and there is no diffuse X-ray scattering. Thus the chains are randomly oriented with respect to one another, with 50% occupation of each of the two inversion-related positions. The Mo atom is displaced by 0.37 Å from the inversion centre, whilst the remainder of the non-H atoms

Table 1 Crystal and refinement data for [BEDT-TTF][$MoOCl_4(H_2O)$] and [BEDT-TTF]$_2$[$Cr(NCS)_4(NH_3)_2$]

	[BEDT-TTF][$MoOCl_4(H_2O)$]	[BEDT-TTF]$_2Cr(NCS)_4(NH_3)_2$
Chemical formula	$C_{10}H_{10}Cl_4MoO_2S_8$	$C_{24}H_{22}CrN_6S_{20}$
M	656.4	1087.7
Crystal system	Triclinic	Monoclinic
Space group	$P\bar{1}$	*C*2/*c*
a/Å	6.174(2)	33.326(9)
b/Å	8.989(4)	5.778(1)
c/Å	10.103(4)	23.737(5)
α/°	71.95(3)	
β/°	79.24(3)	115.07(2)
γ/°	83.77(3)	
U/Å^3	523.0(4)	4140(2)
Z	1	4
F(000)	324	2208
D_c/g cm^{-3}	2.08	1.74
Crystal size/mm	0.12 × 0.12 × 0.40	0.06 × 0.40 × 0.50
μ(Mo-Kα)/cm^{-1}	19.0	12.7
Data measured	2029	4914
Unique data	1845	3607
No. data with $I \geqslant 4\sigma(I)$	1466	2526
No. parameters	130	230
Absorption correction	Empirical	—
μ*R*	0.24	—
Minimum, maximum transmission	0.66, 0.76	—
R (all data)	0.038 (0.0525)	0.057 (0.087)
R′	0.033	0.059
g (weighting)	0.00	7.08 × 10^{-4}
Largest peak/e Å^{-3}	0.5, −0.4	0.6, −0.7

Table 2 Selected bond lengths (Å) and angles (°) for [BEDT-TTF][$MoOCl_4(H_2O)$]

Mo–Cl(1)	2.360(2)	Mo–O(1)	1.631(4)
Mo–Cl(2)	2.320(2)	Mo–O(1A)	2.372(4)
Mo–Cl(1A)	2.373(2)	O(1)–H(5)	0.835(4)
Mo–Cl(2A)	2.403(2)		
S(1)–C(1)	1.708(6)	C(1)–C(1A)	1.386(10)
S(1)–C(2)	1.724(5)	C(2)–C(3)	1.342(7)
S(2)–C(1)	1.710(5)	C(4)–C(5)	1.471(9)
S(2)–C(3)	1.732(6)	C(4)–H(1)	1.09(7)
S(3)–C(2)	1.749(6)	C(4)–H(2)	0.82(8)
S(3)–C(4)	1.828(7)	C(5)–H(3)	0.93(6)
S(4)–C(3)	1.735(5)	C(5)–H(4)	1.06(7)
S(4)–C(5)	1.800(8)		
Cl(1)–Mo–Cl(2)	90.0(1)	Cl(1)–Mo–O(1)	99.1(2)
Cl(2)–Mo–Cl(1A)	89.1(1)	Cl(2)–Mo–O(2)	100.4(1)
Cl(1)–Mo–Cl(1A)	161.9(1)	Mo–O(1A)–H(5A)	116.6(3)
Cl(2)–Mo–Cl(2A)	161.9(1)		

approximate inversion symmetry and were refined anisotropically with 100% occupation. Of the eight previously reported salts of this anion found in the Cambridge Crystallographic Database none exhibits hydrogen-bonded chains and none shows disorder of the anion about an inversion centre. The geometry found agrees with those previously reported.

Electron-transfer integrals between the nearest-neighbour BEDT-TTF are negligible except for the side-to-side interaction along the *a* axis. The calculation therefore predicts a half-filled one-dimensional cosinal band along *a**, although with only a moderate transfer integral along the ribbons ($t' = 165$ meV) there is a likelihood that Coulombic repulsion may dominate giving rise to the Mott–Hubbard insulating ground state. The only other BEDT-TTF salt which contains a uniform linear ribbon of BEDT-TTF is [BEDT-TTF][$Re_6Se_5Cl_9$]·2dmf [8,9] in which the donor array behaves as a one-dimensional antiferromagnet, *i.e.* as a Mott–Hubbard insulator.

[BEDT-TTF]$_2$[$Cr(NCS)_4(NH_3)_2$]. This phase is one of the few BEDT-TTF charge-transfer salts to crystallise in the monoclinic space group *C*2/*c*. The asymmetric unit contains one BEDT-TTF molecule and one half of the $[Cr(NCS)_4(NH_3)_2]^-$ on the (0, 0, 0) inversion centre. The eight symmetry operations generate two equivalent non-chiral BEDT-TTF layers, each

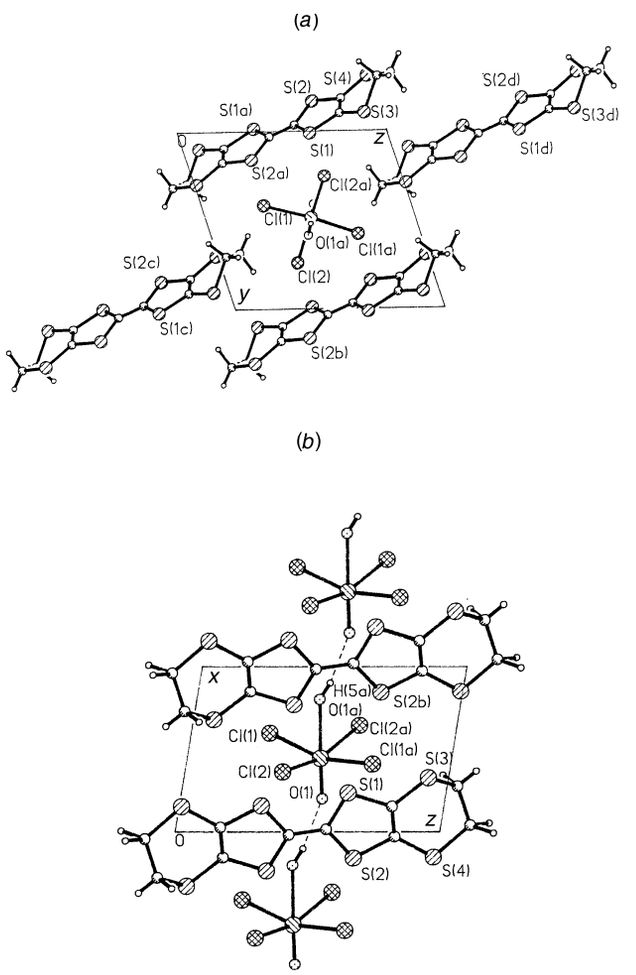

Fig. 1 Projection of the crystal structure of [BEDT-TTF][$MoOCl_4(H_2O)$], (*a*) down the *a* axis and (*b*) down the *b* axis (for clarity only one orientation of the anion is shown)

Table 3 Selected intramolecular bond lengths (Å) and angles (°) for $[BEDT\text{-}TTF]_2[Cr(NCS)_4(NH_3)_2]$

Cr–N(11)	1.981(5)	N(12)–C(12)	1.153(9)
Cr–N(12)	1.996(6)	C(11)–S(11)	1.613(7)
Cr–N(13)	2.069(7)	C(12)–S(12)	1.606(7)
N(11)–C(11)	1.161(9)		
S(1)–C(1)	1.743(6)	S(4)–C(2)	1.736(6)
S(1)–C(3)	1.737(6)	S(4)–C(6)	1.750(5)
S(2)–C(1)	1.736(6)	C(1)–C(2)	1.355(7)
S(2)–C(4)	1.745(6)	C(3)–C(4)	1.352(10)
S(3)–C(2)	1.736(6)	C(5)–C(6)	1.344(9)
S(3)–C(5)	1.747(6)		
N(11)–Cr–N(12)	88.9(2)	N(12)–Cr–N(13)	90.0(2)
N(11)–Cr–N(13)	89.1(2)		

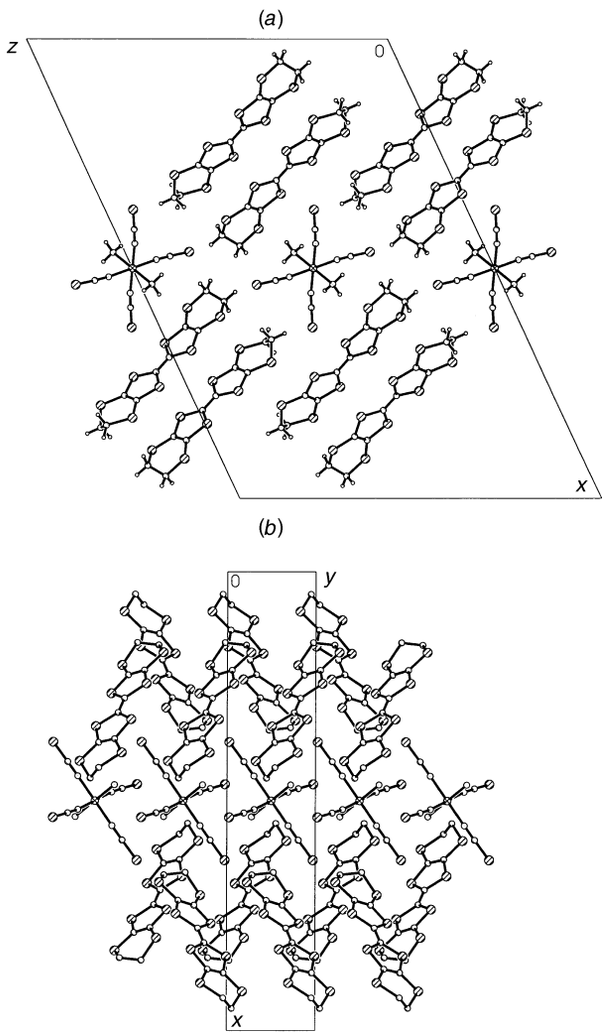

Fig. 2 Projection of the crystal structure of $[BEDT\text{-}TTF]_2[Cr(NCS)_4(NH_3)_2]$, (*a*) down the *b* axis and (*b*) down the *c* axis (hydrogen atoms are omitted for clarity)

containing four discrete molecules in the repeat unit. Alternating layers of $[(BEDT\text{-}TTF)_2]^+$ and $[Cr(NCS)_4(NH_3)_2]^-$ propagate along the *a* direction (Fig. 2). The atomic numbering scheme is given in Fig. 3. Selected intramolecular bond lengths and angles are listed in Table 3, and the shortest intermolecular S···S distances may be found alongside the calculated intermolecular transfer integrals in Table 4.

The packing of the BEDT-TTF layer is a novel one among this class of charge-transfer salts, with double stacks which alternate in orientation (Fig. 4). The double stacks propagate

Table 4 Transfer integrals (t') and intermolecular S···S distances of $[BEDT\text{-}TTF]_2[Cr(NCS)_4(NH_3)_2]$

		S···S ≤4.0 Å		
	t'/meV	Inner–inner	Inner–outer	Outer–outer
A	200	3.76, 3.91, 3.93	3.60, 3.68	3.75, 3.82
B	26	3.70, 4.00	—	—
C	86	3.83, 4.01	3.66	3.51
D	7	—	3.710	—

'Inner' and 'outer' denote S atoms of the TTF and ethylenedithiomoieties respectively. For definitions of A–D see Fig. 4.

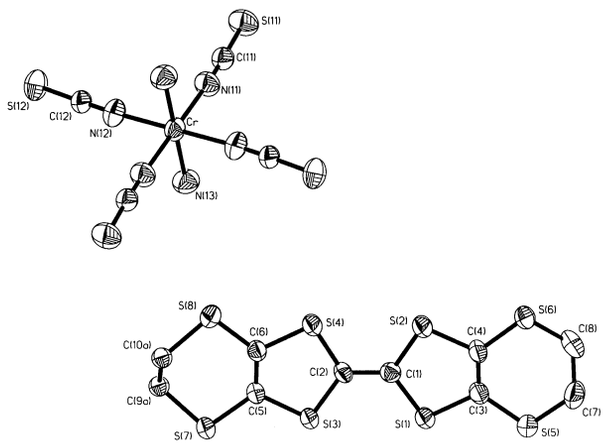

Fig. 3 Atomic numbering scheme of $[BEDT\text{-}TTF]_2[Cr(NCS)_4(NH_3)_2]$ (showing 50% thermal ellipsoids)

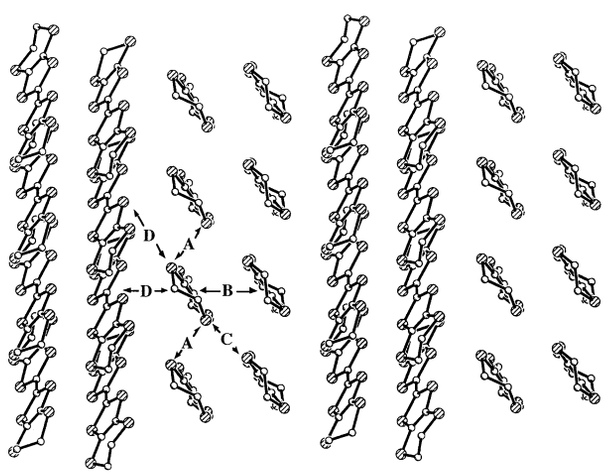

Fig. 4 Projection of the BEDT-TTF layer of $[BEDT\text{-}TTF]_2[Cr(NCS)_4(NH_3)_2]$ down the long molecular axes; A–D denote the four independent intermolecular interactions

along *b* and are slipped and canted with respect to one another along *c* in such a way that the packing is therefore highly one-dimensional. Other BEDT-TTF salts reported to crystallise in the space group *C*2/*c* include η-$[BEDT\text{-}TTF]_2[Au(CN)_2]$[11] and $[BEDT\text{-}TTF]_4[Hg_3I_8]$.[12] The packing arrangement in the latter is quite different but the structures of η-$[BEDT\text{-}TTF]_2[Au(CN)_2]$ and $[BEDT\text{-}TTF]_2[Cr(NCS)_4(NH_3)_2]$, which have similar unit-cell dimensions, are quite similar. In the gold salt the smaller area of the *bc* plane (94.1 Å^2 compared to 137.2 Å^2 for the chromium salt) means that the BEDT-TTF molecule is nearly perpendicular to the layer, resulting in a truly two-dimensional interacting network. The larger area of the *bc* plane in $[BEDT\text{-}TTF]_2[Cr(NCS)_4(NH_3)_2]$ arises not from the increased size of the anion, but from the effects of inter-

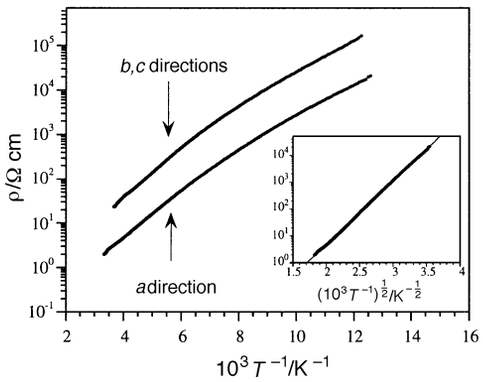

Fig. 5 Electrical transport of [BEDT-TTF][$MoOCl_4(H_2O)$]. The inset is a fit by a one-dimensional hopping model

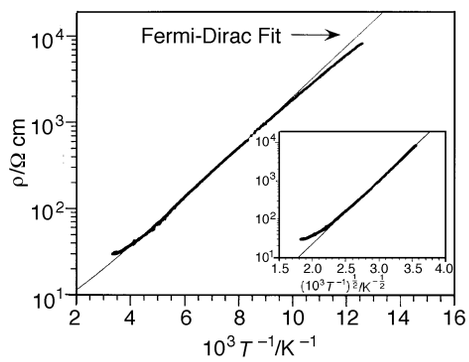

Fig. 6 Electrical transport of [BEDT-TTF]$_2$[$Cr(NCS)_4(NH_3)_2$]. The straight line is a fit by a coherent semiconductor model, the inset a fit by a one-dimensional hopping model

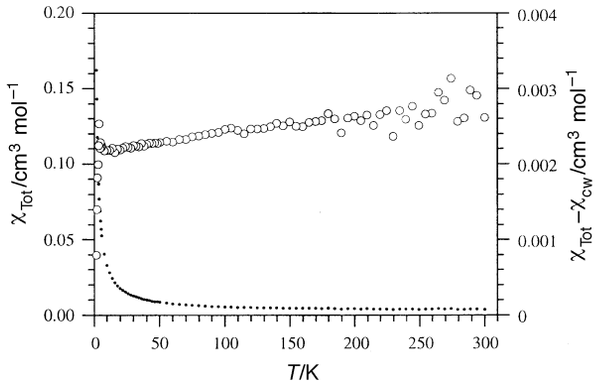

Fig. 7 Temperature-dependent susceptibility of [BEDT-TTF][$MoOCl_4(H_2O)$]. The dots indicate total susceptibility and open circles that after subtracting a Curie–Weiss contribution (see text)

molecular forces: the NH_3 lies far from the CH_2 groups of the BEDT-TTF, whilst the S···S and H···S interactions are maximised.

In addition to many short S···S distances within the double ribbons, and one between ribbons (Table 4), there are several between the cations and anion, *e.g.* from the thiocyanate S(11) to inner BEDT-TTF S the distances are 3.68, 3.78 and 3.84 Å, and from S(12) and S(11) to outer BEDT-TTF S the distances are 3.44 and 3.88 Å respectively. The long axis of the BEDT-TTF makes an angle of 45.0° to the layer because one of the anion NCS groups penetrates into the cation layer. Both terminal CH_2 groups of the BEDT-TTF adopt the chair form, one being disordered, so that the molecule has *ca.* 55% occupation of the eclipsed conformation and 45% occupation of the staggered.

The symmetry of the BEDT-TTF layer requires that two of the six nearest-neighbour intermolecular interactions are equivalent (Fig. 4). Electronic transfer integrals (Table 4) are dominated by the edge-to-edge interaction A within the corrugated ribbons of BEDT-TTF though these are significant for the other two interactions B and C, but negligible for the interaction between the ribbons of molecules the axes of which are not parallel (D). This suggests that the BEDT-TTF layer can be considered as consisting of double chains of parallel molecules along the *b* axis, canted with respect to neighbouring chains, and electronically isolated from each other. The dominance of the A interaction over B and C suggests there may be delocalisation of charge along the BEDT-TTF chains, rather than Mott–Hubbard localisation on neighbouring [$(BEDT\text{-}TTF)_2$]$^+$.

Electrical conductivity

The salt [BEDT-TTF][$MoOCl_4(H_2O)$] is semiconducting, with a temperature-dependent energy of activation energy E_A ranging from 0.21 eV at 300 K to 0.08 eV at 100 K (Fig. 5). The room-temperature conductivities are quite high for a salt of BEDT-TTF$^+$: σ_{RT}(*a* direction) − 0.5, (*b*,*c* directions) ≈ 0.05 S cm^{-1}. The decreasing E_A with cooling is reminiscent of many one-dimensional conducting materials, and is consistent with the one-dimensional electron-hopping model [13] (inset to Fig. 5).

The salt [BEDT-TTF]$_2$[$Cr(NCS)_4(NH_3)_2$] is likewise semiconducting, with a temperature-dependent E_A and a room-temperature conductivity σ_{RT}(*b* direction) ≈ 30 S cm^{-1} (Fig. 6). The behaviour is strongly reminiscent of other one-dimensional materials, *e.g.* $K_2[Pt(CN)_4]Br_{0.30}\cdot 3H_2O$. At high temperature there is a reproducible upturn in the resistivity which exceeds that predicted by Fermi–Dirac statistics, and may therefore indicate a transition towards the metallic state. Below this feature there is a gradual decrease in E_A from 56 meV at 300 K to 41 meV at 80 K. The low-temperature behaviour is closely modelled by the one-dimensional hopping law (inset to Fig. 6), suggesting that the material may be semiconducting due to Mott–Hubbard localisation.

Magnetic susceptibility

The magnetic properties of [BEDT-TTF][$MoOCl_4(H_2O)$] are dominated by the $S = \frac{1}{2}$ Curie–Weiss behaviour of the d^1 anion, with $C = 0.32(2)$ cm^3 K mol^{-1} [$g = 1.85(5)$], $\theta = -0.22$ K. The comparatively large Weiss constant {*cf.* $\theta = -0.003$ K for [NEt_4][$MoOCl_4(H_2O)$]} probably results from antiferromagnetic superexchange *via* the hydrogen bonding. The susceptibility remaining after subtraction of the Curie–Weiss component (shown as open circles in Fig. 7) is larger than that for [NEt_4][$MoOCl_4(H_2O)$] by *ca.* 10^{-3} cm^3 mol^{-1}, and has a subtly different temperature dependence, consistent with an antiferromagnetic contribution from the BEDT-TTF$^+$ chains, with $J \approx 110$ K.

The magnetic properties of [BEDT-TTF]$_2$[$Cr(NCS)_4(NH_3)_2$] are dominated by the Curie-type susceptibility of the d^3, $S = \frac{3}{2}$ anion. The shape of the residual susceptibility is sensitive to small variations in the diamagnetic correction and on the molar quantity (*n*), each of which have large errors due to the small sample mass.

Subtraction of the component of susceptibility due to the anions was performed using the Brillouin function, since there is a considerable degree of spin saturation at low temperature. The residual susceptibility assigned to the cations could not be successfully modelled as the sum of Curie–Weiss and Bonner–Fisher [14] (linear antiferromagnetic chain) components, nor are they described by the sum of Curie–Weiss and $T^{-\alpha}$ (defect susceptibility) components. The large magnitude and negative sign of the residual susceptibility suggests it results primarily from a temperature-dependent moment of the anion. The data analyses presented in Figs. 8 and 9 were performed assuming $\theta = 0.0$ K and $n = 100\%$.

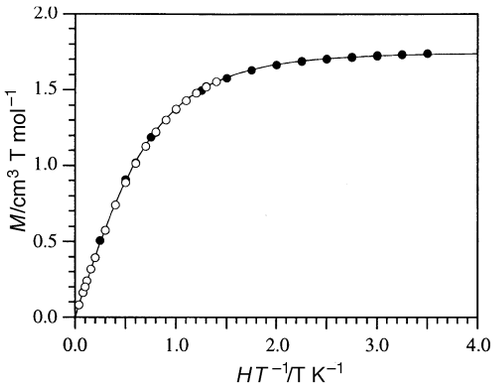

Fig. 8 Magnetisation of $[BEDT\text{-}TTF]_2[Cr(NCS)_4(NH_3)_2]$ at 2 (●) and 5 K (○). The line is a fit by a Brillouin function with $S = \frac{3}{2}$, $\theta = 0$ K, $g = 2.08$

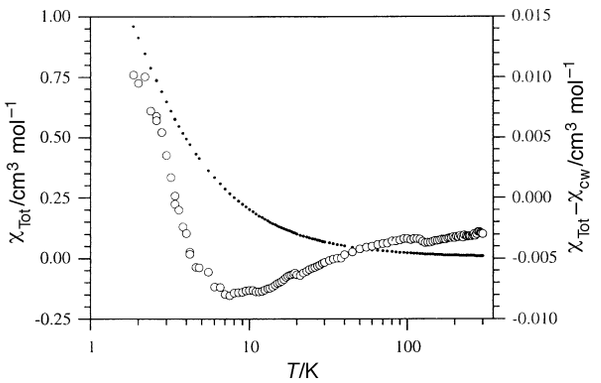

Fig. 9 Temperature-dependent susceptibility of $[BEDT\text{-}TTF]_2[Cr(NCS)_4(NH_3)_2]$. Filled circles represent the total susceptibility, open circles that after subtracting a Curie component (see text)

Infrared reflectivity

Crystals of $[BEDT\text{-}TTF]_2[MoOCl_4(H_2O)]$ have a reflectivity lower than 30% in the range 700–4300 cm^{-1}, characteristic of a semiconductor. The reflectance along *a* (parallel to the cation chains) is approximately double the perpendicular reflectivity, indicating that the band structure is highly one-dimensional. Vibrational peaks occur at 755 [ν(Mo–O)], 784 [ν(C–S)], 900, 974 [$\nu(Mo^{V}{=}O)$, compared to reported values of 985 and 992], 1023, 1180 and 1582 cm^{-1} [δ(H–O–H)]. The observation of the H_2O bending mode confirms the proposed stoichiometry of the anion. From the perpendicular measurements vibrational peaks occur at 881, 1259, 1328, 1413 and 1425 cm^{-1} [ν(C=C)].

The infrared reflectance spectra of $[BEDT\text{-}TTF]_2[Cr(NCS)_4(NH_3)_2]$ are similar to those of a metal, with moderately high reflectivities, and a feature of 1385(5) cm^{-1} arising from the donor ν(C=C) mode broadened by interaction with delocalised conduction electrons. There is a three-fold difference in reflectance for polarisation parallel and perpendicular to the *b* direction, again indicating that the band structure is strongly one-dimensional. Several sharp vibrational peaks were found, the most prominent, near 2078 cm^{-1}, arising from the ν(CN) mode of the NCS parallel with the BEDT-TTF plane.

Conclusion

Two new semiconducting BEDT-TTF charge-transfer salts have been structurally and physically characterised, each with highly unusual one-dimensional molecular packing. The unit cells of $[BEDT\text{-}TTF][MoOCl_4(H_2O)]$ and $[BEDT\text{-}TTF]_2[Cr(NCS)_4(NH_3)_2]$ each contain only one crystallographically independent BEDT-TTF. The structure of the former contains isolated edge-linked ribbons of $BEDT\text{-}TTF^{+}$ while the latter contains discrete layers containing double ribbons of $BEDT\text{-}TTF^{0.5+}$ that are canted with respect to one another.

The temperature-dependent electrical conductivity does not provide an unambiguous means of determining the electronic origin of the observed semiconducting behaviour. Understanding of the magnetic properties is required to remove this uncertainty but for both compounds the large temperature-dependent moments of the anions make it difficult to determine the contribution from the BEDT-TTF sublattice.

The residual susceptibility assigned to the $BEDT\text{-}TTF^{+}$ ribbons in the molybdenum salt is consistent with one-dimensional antiferromagnetic (Bonner–Fisher) behaviour with an exchange constant of the magnitude expected from the intrachain transfer integral. Infrared reflectance spectra are characteristic of the semiconducting state, suggesting that disorder of the anion chains is not the cause of the semiconductivity. The absence of X-ray satellite reflections at room temperature and the high-temperature semiconducting behaviour disfavour the two forms of electronic modulation. Coulombic repulsion is important for the half-filled band, since electronic transfer requires the process $2BEDT\text{-}TTF^{+} \longrightarrow BEDT\text{-}TTF^{2+} + BEDT\text{-}TTF^{0}$. The material may therefore be characterised as a Mott–Hubbard insulator. The electrical transport is consistent with one-dimensional variable-range hopping. The room-temperature conductivities are comparatively high for a salt of $BEDT\text{-}TTF^{+}$, attributable to the large intrachain transfer integral.

It is not clear whether long-range electronic delocalisation occurs in $[BEDT\text{-}TTF]_2[Cr(NCS)_4(NH_3)_2]$, since determination of the cation contribution to the magnetic susceptibility requires a better knowledge of the magnetic behaviour of the distorted-octahedral anion. In contrast to $[BEDT\text{-}TTF][MoOCl_4(H_2O)]$, the BEDT-TTF carry a partial charge. The highly anisotropic transfer integrals suggest that there is delocalisation along the double cation chains rather than Mott–Hubbard localisation on each pair of cations. The polarised infrared reflectance spectra indicate a high degree of anisotropy in the band structure, with polarisation parallel with the double cation ribbons showing optical properties characteristic of a metal. The electrical transport properties have a similar form to many one-dimensional materials which are metallic at high temperature and undergo transition to a charge density wave (CDW)-modulated semiconducting state. The very small activation energies of electrical transport are atypical of the Mott–Hubbard insulating state, since pressure is generally expected to increase transfer integrals to stabilise the metallic band. No X-ray satellite reflections were observed at room temperature, although a CDW structural modulation with a transition temperature in the vicinity of 300 K cannot be ruled out.

In conclusion, the origin of the semiconducting behaviour of these two compounds with two different average cation charges and novel molecular packing is complex, but the field of structure–property relations in the BEDT-TTF series of charge-transfer has been further enlarged.

Acknowledgements

We acknowledge the UK Engineering and Physical Sciences Research Council and the European Union (Human Capital and Mobility Programme) for financial support. C. J. K. thanks the University of Western Australia for a Hackett Scholarship. We are grateful to Dr. W. Hayes (Clarendon Laboratory, Oxford) for access to the infrared spectrometer, and Dr. P. Guionneau and L. Ducasse for assistance with the band-structure calculations.

References

1 P. Day, in *Solid State Chemistry: Compounds*, eds. A. K. Cheetham and P. Day, Clarendon Press, Oxford, 1992, pp. 31–59.

2 E. Conwell (Editor), *Semiconductors and Semimetals: Highly Conducting Quasi-one-dimensional Organic Crystals*, Academic Press, New York, 1988.
3 K. Krogmann, *Angew. Chem., Int. Ed. Engl.*, 1969, **8**, 35.
4 T. J. Marks, *Angew. Chem., Int. Ed. Engl.*, 1990, **29**, 857.
5 A. Bino and F. A. Cotton, *Inorg. Chem.*, 1979, **18**, 2710.
6 G. M. Sheldrick, SHELXTL PLUS, Version 4.2, Siemens Analytical X-Ray Instruments Inc., Madison, WI, 1990.
7 A. Kawamoto, J. Tanaka and M. Tanaka, *Acta Crystallogr., Sect. C*, 1987, **43**, 205.
8 A. Pénicaud, C. Lenoir, P. Batail, C. Coulon and A. Perrin, *Synth. Met.*, 1989, **32**, 25.
9 A. Pénicaud, K. Boubekeur, P. Batail, C. Canadell, P. Auban-Senzier and D. Jérome, *J. Am. Chem. Soc.*, 1993, **115**, 4101.
10 L. C. Potter, H. H. Wang, M. A. Beno, K. D. Carlson, C. M. Pipan, R. B. Proksch and J. M. Williams, *Solid State Commun.*, 1987, **64**, 387.
11 E. Amberger, H. Fuchs and K. Polborn, *Synth. Met.*, 1987, **19**, 605; M. Kurmoo, P. Day, T. Mitani, H. Kitagawa, H. Shinoda, D. Yoshida, P. Guionneau, Y. Barrans, D. Chasseau and L. Ducasse, *Bull. Chem. Soc. Jpn.*, 1996, **69**, 1223.
12 M. Z. Aldoshina, L. M. Goldenberg, R. N. Lyubovskaya, T. G. Takhirov, O. A. Dyachenko, L. O. Atovmyan, V. A. Merzhanov and R. B. Lyubovskii, *Mater. Sci.*, 1988, **14**, 53.
13 N. F. Mott, *Philos. Mag.*, 1969, **19**, 835.
14 J. C. Bonner and M. E. Fisher, *Phys. Rev. A.*, 1964, **135**, 640.

Received 2*nd September* 1996; *Paper* 6/06025K